SIMULATION OF LARGE INDUSTRIAL OUTDOOR FIRES

Howard R. Baum and Kevin B. McGrattan
National Institute of Standards and Technology
Building and Fire Research Laboratory
Gaithersburg, MD 20899

Abstract

A methodology for simulating the dynamics of large industrial fires in the outdoor environment is presented. The large eddy simulation techniques developed by the authors and their collaborators are used to simulate a fire on top of a large oil storage tank adjacent to several neighboring tanks. The radiative heat transfer to the tanks is estimated as a function of the relative position of the tanks and the degree of shielding provided by the tanks from the ambient wind field and atmospheric stratification. This example is used to outline the issues that must be addressed in order to make a realistic assessment of the hazards generated by large industrial fires.

1. INTRODUCTION

Large outdoor fires can be conveniently divided into two categories based on the fuel source. Wildland fires are characterized by a relatively low heat release rate per unit area of ground covered by fuel, but a very large area over which the fire can spread. Indeed, the description of the fire spread process is an essential part of any successful simulation of such an event. Industrial fires, in contrast, are usually much more highly localized but intense emitters of heat, smoke, and other combustion products. This is particularly true if the fuel is a petroleum based substance, with a high energy density and sooting potential. This latter type of fire is the object of study in the present paper.

The hazards associated with such fires occur on two widely separated length scales. Near the fire, over distances comparable to the flame length, the radiant energy flux can be sufficiently high to threaten both the structural integrity of neighboring buildings, and the physical safety of firefighters and plant personnel. At much greater distances, typically several times the plume stabilization height in the atmosphere, the smoke and gaseous products generated by the fire can reach the ground in concentrations that may be unacceptable for environmental reasons. The far field hazard has been studied previously by the present authors [1], [2]. This work has led to the development of a computer code ALOFT, which is available from NIST. A comprehensive description of ALOFT and its generalizations to complex terrain can be found in [3].

In this paper the near field hazard associated with the flame radiation is studied. The scenario chosen is a fire on top of an oil storage tank adjacent to several neighboring tanks. This scenario is chosen both for its intrinsic importance and because it illustrates the ingredients needed to generate a realistic simulation of such an event. The heat release generated by a fire on this scale can reach several gigawatts if the entire pool surface is exposed and burning. Such fires interact strongly with the local topography (both natural and man made) and the vertical distribution of wind and temperature in the atmosphere. Moreover, the phenomena are inherently

Fire Detection, Fire Extinguishment and Fire Safety Engineering. NRIFD 50th Anniversary Symposium. Proceedings. Fire Fighting Future 50th Session (FFF50th). Organized by National Research Institute of Fire and Disaster (NRIFD) and Fire and Disaster Management Agency (FDMA) and Sponsored by Fire Protection Equipment and Safety Center. June 1, 1998, Tokyo, Japan, 23-30 pp, 1998

time dependent and involve a wide temperature range. Thus, the simplifications employed in ALOFT and its generalizations can not be used in the present analysis.

In the next section a model is presented that contains the basic components needed to address this problem. The model consists of a version of the authors three dimensional enclosure fire model [4], [5] modified to account for a stratified atmosphere. This is supplemented by a simple radiative tranport model that ignores the absorption by the smoke generated in the fire. The effect of the absorption is accounted for by lowering the radiant energy emission from the flames. The atmospheric boundary layer wind is represented by a power law velocity profile and the ambient temperature fields are taken to be isothermal. The resulting radiant heat flux incident on the tank surfaces are shown in the third section. The implications of these results for both storage tank safety and the utility of this methodology in general are discussed.

2. OUTDOOR FIRE MODEL

The starting point is the equations of motion for a compressible flow in the low Mach number approximation. However, the equations as developed by Rehm and Baum [6] must be modified to allow for an ambient pressure $P_0(z)$, temperature $T_0(z)$ and density $\rho_0(z)$ that vary with height z in the atmosphere in the absence of the fire. Their equations assume that the fire induced pressure is a small perturbation about the time dependent spatial average of the pressure in an enclosure. For the present application, the fire induced pressure $\tilde{p}$ is a small perturbation about $P_0(z)$. The ambient density and temperature are related to $P_0(z)$ by the equation of state and the assumption of hydrostatic balance in the ambient atmosphere. The equations expressing the conservation of mass, momentum, and energy then take the form:

$$\frac{D\rho}{Dt} + \rho \nabla \cdot \vec{u} = 0 \tag{1}$$

$$\rho \left(\frac{\partial \vec{u}}{\partial t} - \vec{u} \times \vec{\omega} + \nabla \left(\frac{1}{2} u^2 \right) \right) + \nabla \tilde{p} - (\rho - \rho_0)\, \vec{g} = \nabla \cdot \tau \tag{2}$$

$$\rho\, C_p \frac{DT}{Dt} - w \frac{dP_0}{dz} = \nabla \cdot \vec{q} + Q_c \tag{3}$$

Here, ρ is the density, $\vec{u}$ the velocity, T the temperature, and $\tilde{p}$ the fire induced pressure in the gas. The unresolved momentum flux and viscous stress tensors are lumped together and denoted by τ. The quantity $\vec{\omega}$ is the fluid vorticity. The vertical component of the velocity is denoted by w in equation (3) and the hydrostatic relation between P_0 and ρ_0 has been used in equation (2). The specific heat is denoted by C_p. Similarly, the unresolved advected energy flux, the conduction heat flux, and the radiant energy flux are denoted by $\vec{q}$, while the chemical heat release per unit volume is Q_c. These equations are supplemented by models for $\tau, \vec{q}$, and an equation of state:

$$P_0\,(z) = \rho \mathcal{R} T \tag{4}$$

The energy and momentum equations can be thought of as advancing the time evolution of the temperature and velocity respectively. However the pressure perturbation does not obey an explicit time evolution equation. Instead, it is the solution of an elliptic equation determined by the divergence of a "pseudo-velocity" $\vec{v}$ defined as:

$$\vec{v} = \left(\frac{P_0(z)}{p_\infty}\right)^{\frac{1}{\gamma}} \vec{u} \tag{5}$$

Here, p_∞ is the ambient pressure at a reference height. A linear combination of the energy and mass conservation equations can be formed to yield the following equation for the divergence of $\vec{v}$:

$$\nabla \cdot \vec{v} = \frac{\gamma - 1}{\gamma p_\infty} \left(\frac{P_0(z)}{p_\infty}\right)^{-\left(\frac{\gamma-1}{\gamma}\right)} \left(\nabla \cdot \vec{q} + Q_c\right) \tag{6}$$

Note that the pseudo-velocity is indeed a vector in the sense that its transformation rules with respect to changes of coordinates are the same as any other vector quantity. Moreover, the right hand side of equation (6) is nearly the same as that for the enclosure fire case. The sole exception is the appearance of the variable background pressure $P_0(z)$.

The equations presented above also require models for τ and $\vec{q}$, as well as a representation of the heat release from the fire. Details can be found in [4]. Here, attention will be confined to a description of the calculation of the radiant heat flux to the surface. The analysis is based on the assumption that a prescribed fraction of the heat released from each thermal element used to describe the fire is radiated away. This energy is absorbed by any surface it reaches without any attenuation in the gas. For a given point $\vec{r}_s$ on the surface, the radiative flux q_R is given by:

$$q_R = \sum_{i=1}^{N_p} \beta \, \dot{q}_i \, \frac{(\vec{r}_s - \vec{r}_i) \cdot \vec{n}}{4\pi \left|\vec{r}_s - \vec{r}_i\right|^3} \tag{7}$$

The quantity β is the fraction of the thermal energy $\dot{q}_i$ released by the ith element radiated away, $\vec{n}$ is a unit normal to the surface at the point $\vec{r}_s$, and N_p is the total number of radiating elements at the instant in question. Since this number can be in the hundreds of thousands, a suitably weighted random sampling is used to perform the calculation.

3. RESULTS AND DISCUSSION

The mathematical model described above was used to study the radiation heat flux from a fire on top of an oil storage tank to both the burning tank and its immediate neighbors. Figures 1 and 2 display the results of the two simulations performed for this study. A numerical grid consisting of 128 by 128 by 128 cells was used to span a cubic domain 768 m on a side. The cell size was uniformly 6 m by 6 m in the horizontal directions and ranged from 3 m near the ground to 12 m at the top of the cube in the vertical. The diameter of each tank was 84 m, the height 27 m. These tanks were incorporated into the calculation by "blocking" cells. Because boundary layers are not resolvable (except the planetary boundary layer) at this grid resolution, there is little penalty in assuming that the tank walls are not smooth, but rather are saw-toothed. Also, each tank was depressed below ground level and surrounded by an embankment of height 9 m. The geometry of each tank and its associated "trench" are modeled on the oil storage facility of the Japan National Oil Corporation at Tomakomai. However, no attempt was made to simulate the entire facility, which contains over 80 tanks.

A stratified wind profile of the form

$$u(z) = u_0 \left(\frac{z}{z_0}\right)^p \tag{8}$$

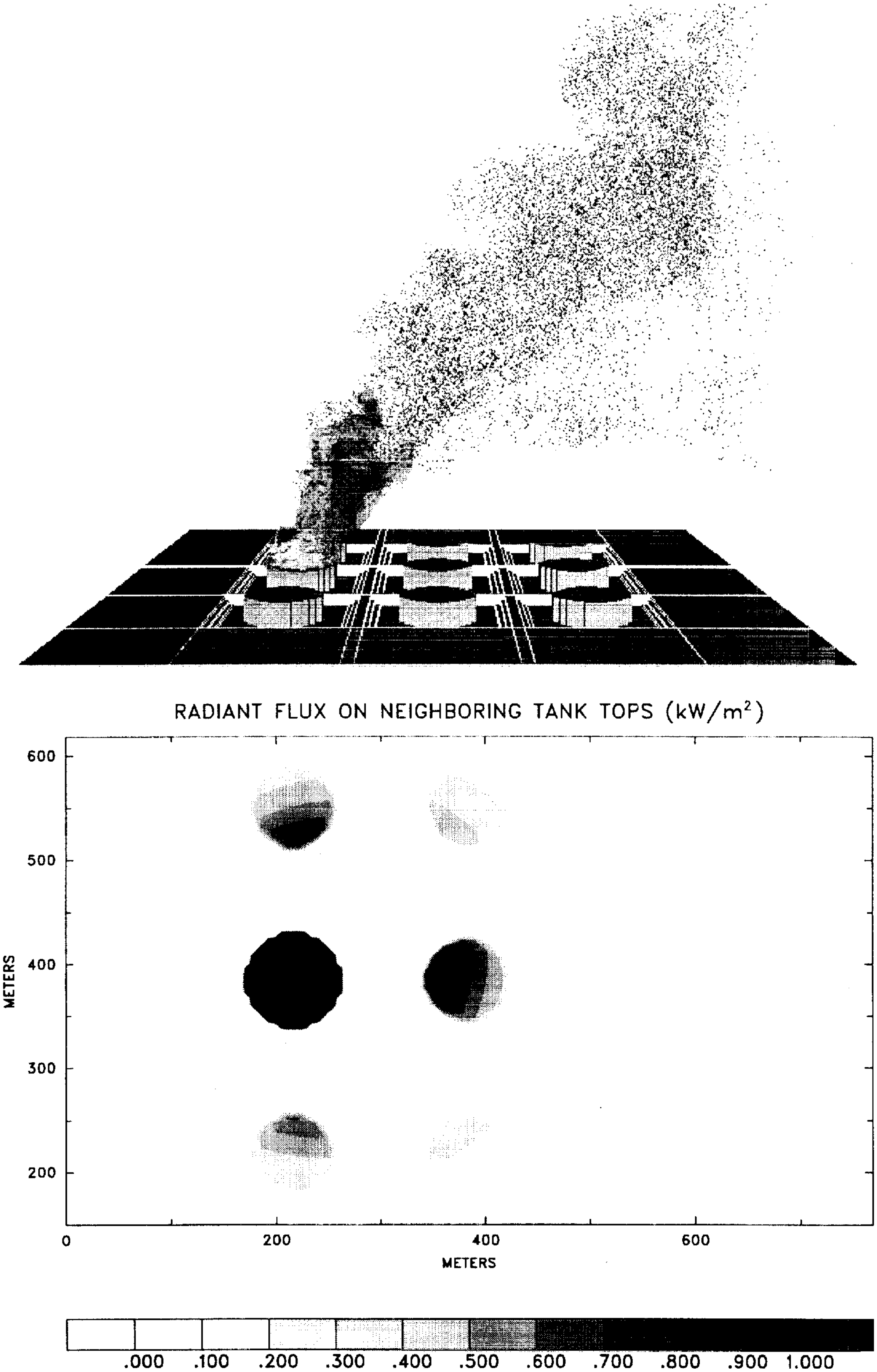

FIGURE 1: Simulation of an oil tank fire. Shown in the top figure are the Lagrangian elements that represent both the fire and the smoke. The bottom figure displays the radiative heat flux from the fire to surrounding tanks.

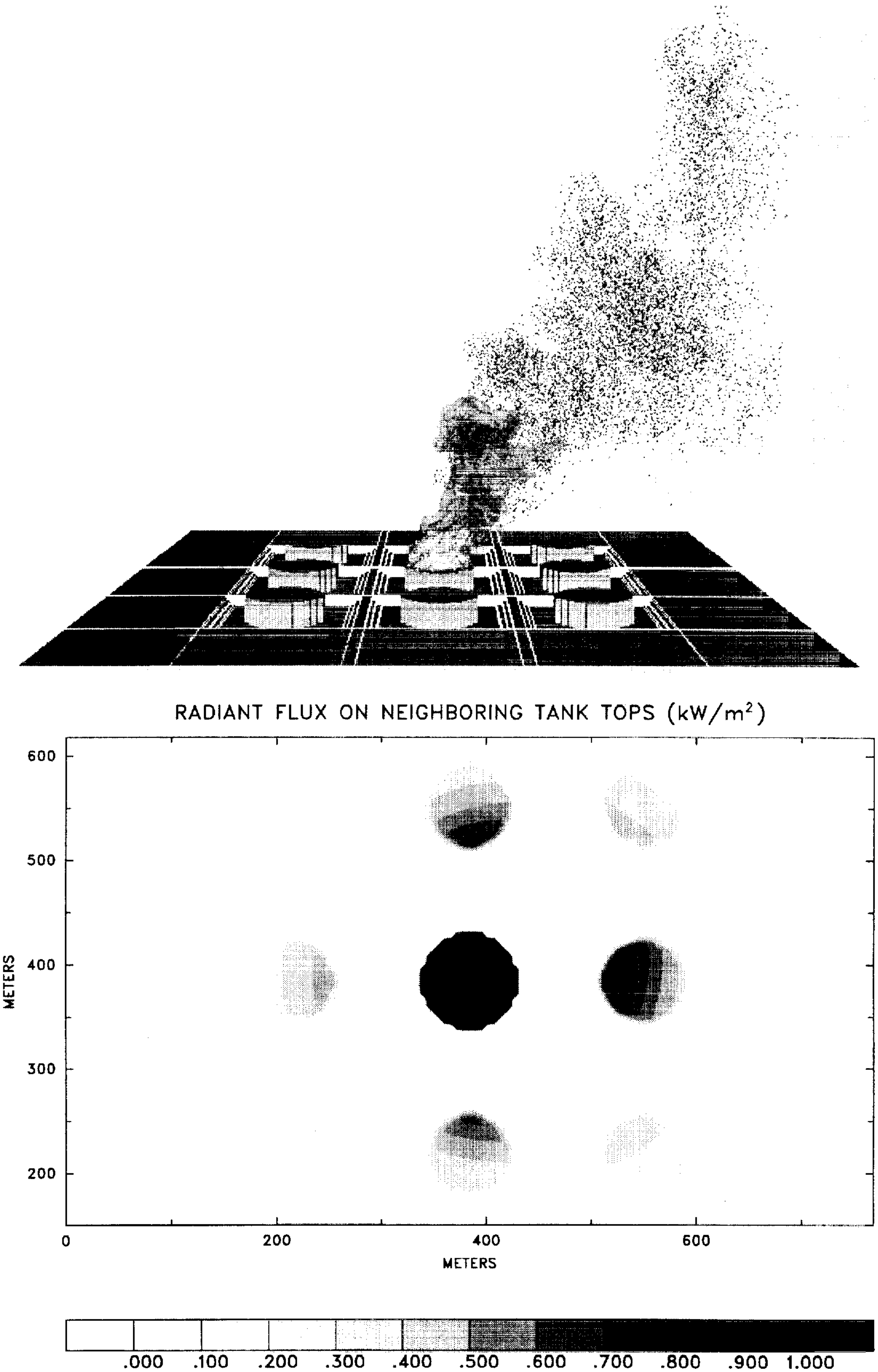

FIGURE 2: Simulation of an oil tank fire. Shown in the top figure are the Lagrangian elements that represent both the fire and the smoke. The bottom figure displays the radiative heat flux from the fire to surrounding tanks.

was imposed as a boundary condition. The wind speed u_0 at a height z_0 of 27 m was 6 m/s. The exponent p, a function of the surface roughness, was 0.15. The temperature of the ambient atmosphere was assumed uniform at 20^oC, although this assumption is not restrictive. The fire was assumed to be engulfing nearly the entire top of the tank, burning with a heat release rate of 1,000 kW/m^2, for a total of 4.7 GW. The fraction of this energy released from the smoke plume as thermal radiation was assumed to be 10% [7]. The radiation heat flux to the neighboring tanks was computed. Figures 1 and 2 show the intensity of radiation on the neighboring tanks for fires in two different locations. Depending on the view factor, the flux on the neighboring tank surfaces ranges from a few tenths to about 2 kW/m^2. On the burning tank itself, the flux back to fuel surface was calculated to be about 18 kW/m^2, but the model of radiation is too crude to account for this feedback reliably. A "$P-1$" radiative transport model incorporating both emission from Lagrangian elements and absorption by the combustion products is currently under development. Note that in the absence of absorption, the flux to any surface scales linearly with radiative fraction.

A comparison of the two figures shows that the radiative flux patterns downwind and to the sides of the burning tank are essentially the same in the two cases. However, the upwind tank in Figure 2 experiences much higher flux levels than the far downwind tank in Figure 1. This is due to the relatively upright fire plume. The radiation is emitted from the shaded region of the fire plume, where the Lagrangian elements are releasing radiant as well as sensible heat. This results in a relatively small view factor for the far downwind tank. The upright plume is caused by the elevation of the fire with respect to the ground, as well as the presence of the tanks as obstacles to the flow. These effects can be seen in Figure 3, which shows velocity vectors near the ground in the vertical centerline plane aligned with the ambient wind. The top figure corresponds to the case with the upwind tank burning, while the lower figure is for the center tank burning. Note that the vortex upwind of the burning center tank is much larger than that ahead of the upwind tank; the latter being confined to the trench. Although all figures in this paper are instantaneous snapshots of the fire, there is good reason to believe that these vortices persist in time, and play a major role in directing the flow around the tanks. The upwind tank does not make a large perturbation to the ambient wind in this plane, because of its partial submergence in the trench and low aspect ratio.

The above examples illustrate the complex interaction between the topography, the ambient atmosphere, and the fire dynamics. Even for the relatively simple configuration chosen for study here, there are many factors that strongly affect the resulting fire dynamics. The ambient wind and temperature fields must play at least as significant a role as they do in the downwind smoke dispersion described by the ALOFT code. The presence of natural topographical features in the vicinity of the storage tanks would further modify the flow patterns, and hence the radiation fields. Finally, the absorption of thermal radiation by the smoke and gaseous combustion products will alter the plume structure by creating distributed energy sources in the flow field. Rather than arbitrarily choosing topograpical, structural, and meteorological features to simulate, it would seem to make more sense to couple the emerging simulation capability to databases that describe the actual built environment and associated topography. Similarly, arbitrary prescriptions of the ambient atmosphere could be replaced with local meteorology simulations based on databases and computer models in use by the weather prediction community. The result would be a simulation capability that could be used routinely to predict the fire hazards resulting from natural or man made disasters in the real world.

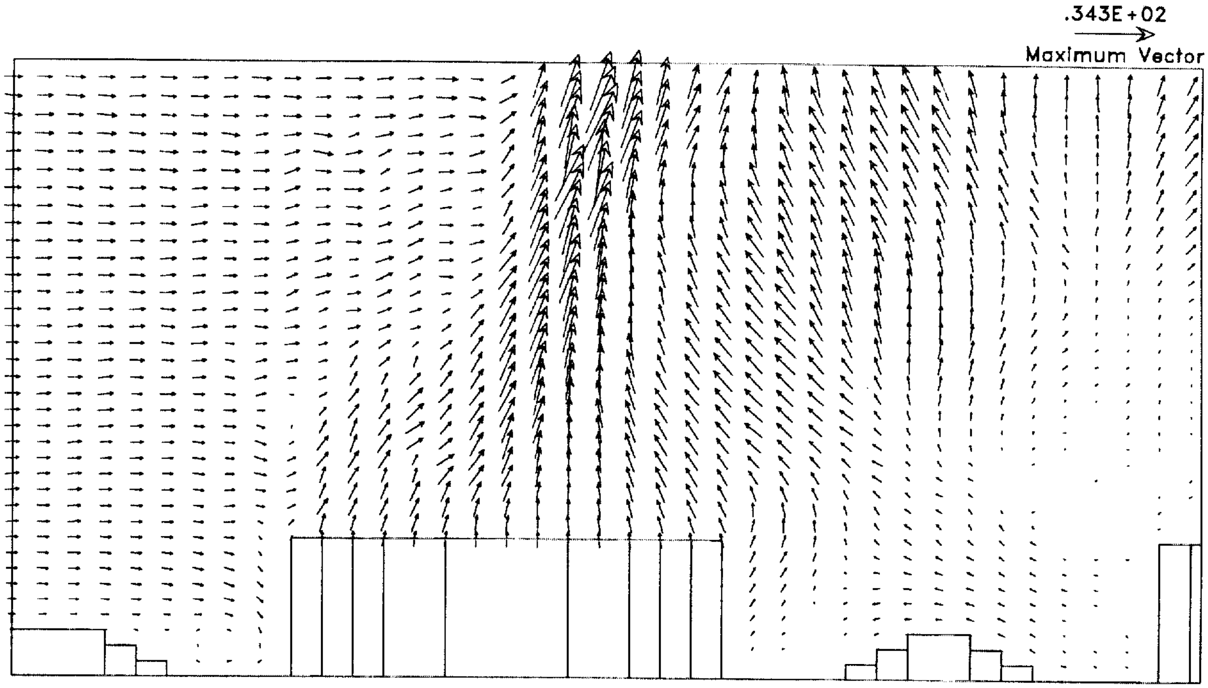

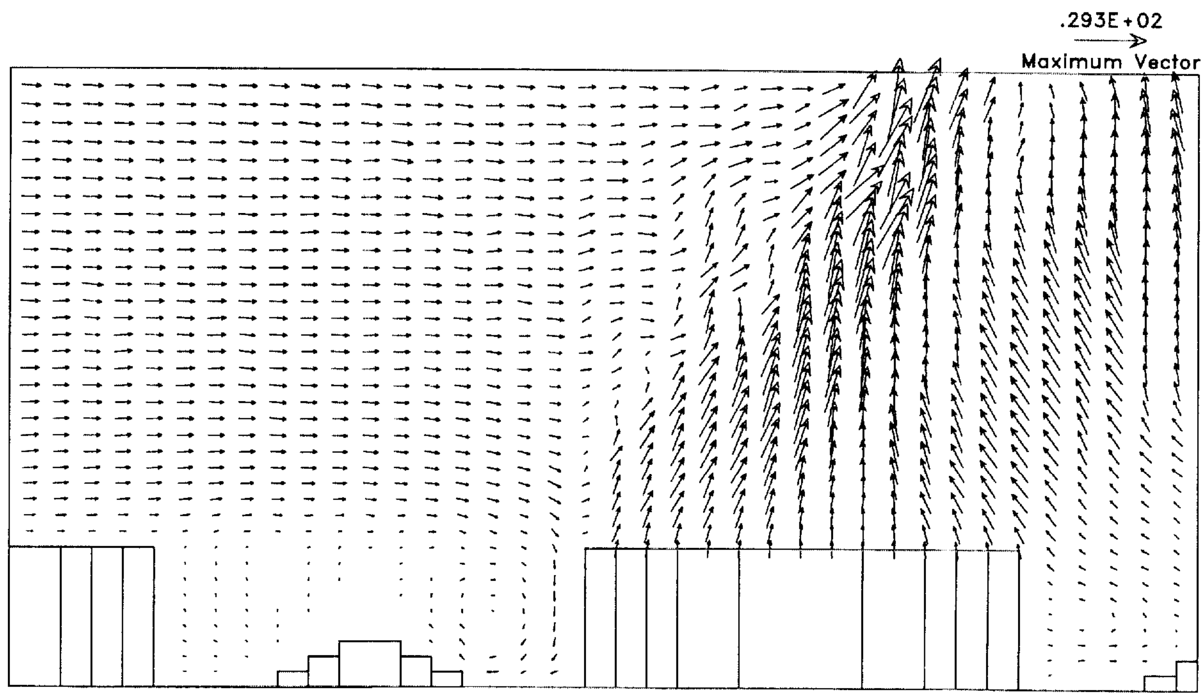

FIGURE 3: Centerline velocity vectors near the base of the fire. The top figure shows the left tank burning, the bottom figure shows the center tank burning.

References

[1] Baum, H.R., McGrattan, K.B., and Rehm, R.G., "Simulation of Smoke Plumes from Large Pool Fires", *Twenty Fifth Symposium (International) on Combustion*, The Combustion Institute, Pittsburgh, pp. 1463-1469, (1994).

[2] McGrattan, K.B., Baum, H.R., and Rehm, R.G., "Numerical Simulation of Smoke Plumes from Large Oil Fires", *Atmospheric Environment*, Vol. 30, pp. 4125-4136, (1996).

[3] McGrattan, K.B., Baum, H.R., Walton, W.D., and Trelles, J., "Smoke Plume Trajectory from In Situ Burning of Crude Oil in Alaska — Field Experiments and Modeling of Complex Terrain", NISTIR 5958, National Institute of Standards and Technology, Gaithersburg, (1997).

[4] Baum, H.R., McGrattan, K.B., and Rehm, R.G., "Three Dimensional Simulation of Fire Plume Dynamics", *Jour. Heat Trans. Soc. Japan*, Vol. 35, pp. 45-52, (1996).

[5] Baum, H.R., McGrattan, K.B., and Rehm, R.G., "Three Dimensional Simulation of Fire Plume Dynamics", *Fire Safety Science - Proceedings of the Fifth International Symposium*, Y. Hasemi, Ed., International Association for Fire Safety Science, pp. 511-522, (1997).

[6] Rehm, R.G. and Baum, H.R., "The Equations of Motion for Thermally Driven, Buoyant Flows", *J. Research of Nat. Bur. Standards*, Vol. 83, pp. 297-308, (1978).

[7] Koseki, H. and Mulholland, G.W., "The effect of diameter on the burning of crude oil pool fires," *Fire Technology*, Vol. 54 (1991).